48th AIAA/ASME/ASCE/AHS/ASC Structures, Structural Dynamics, and Materials Conference
23 - 26 April 2007, Honolulu, Hawaii

AIAA 2007-2055

Time-Frequency based Classification of Structural Damage

Narayan Kovvali[†], Santanu Das[‡], Debejyo Chakraborty[†], Douglas Cochran[†],
Antonia Papandreou-Suppappola[†], Aditi Chattopadhyay[‡]

[†]*Department of Electrical Engineering, Arizona State University, Tempe, Arizona, USA*

[‡]*Department of Mechanical and Aerospace Engineering, Arizona State University, Tempe, Arizona, USA*

The detection and classification of damage in complex materials and structures is essential from both safety and economic perspectives. In this paper, we propose algorithms for the classification of structural damage based on time-frequency techniques. Our approach is based on matching damage features in the time-frequency plane using highly localized Gabor functions and time-varying received signals from real experimental measurements. Example results are presented for the classification of fastener damage in an aluminum plate, demonstrating the utility of the proposed methodology.

Nomenclature

t	time
x	signal
g	MPD dictionary atom
r	residue
α	MPD expansion coefficient
κ	MPD atom width parameter
τ	MPD atom time shift
f	frequency shift
M	number of training signals
Λ	set of all classes
$\mathscr{E}$	cross-term free TFR
WD	Wigner distribution

Subscript
i, j, k indices

I.   Introduction

The detection and classification of damage in complex materials and structures is an important problem encountered in many applications. Examples include the design of aircraft, space navigation vehicles, bridges, buildings, and so on. The primary purpose of damage detection and classification is for the monitoring of structural health, in-time *in situ* diagnosis, and prognosis or residual useful life estimation of key system components.

The inherent complexity of wave propagation in such media, compounded further by its interaction with various external effects, calls for the deployment of advanced signal processing methodologies. Previous effort on structural damage detection and classification has focused on the use of various non-destructive evaluation (NDE) techniques,[1–4] Fourier transform,[5] wavelet-based analysis,[6–8] statistical methods,[9–11] and Lamb waves.[12–15] Many of these methods, however, have disadvantages such as high cost, limited damage detection sensitivity, and high power requirement.

American Institute of Aeronautics and Astronautics

48th AIAA/ASME/ASCE/AHS/ASC Structures, Structural Dynamics, and Materials Conference
23 - 26 April 2007, Honolulu, Hawaii

AIAA 2007-2055

In this paper, we will present two algorithms for the classification of structural damage based on matching pursuit decompositions (MPD)[16–18] and time-frequency representations (TFRs).[19] The MPD algorithm allows for the representation of a signal in terms of a set of *custom-built* basis functions. Since the basis functions used are fine-tuned to the signal type in question, it follows that the MPD yields a signal representation that is very compact; in fact, the MPD is especially useful for the extraction of specific features of interest and rejection of unwanted signal components such as noise. Time-frequency representations (TFRs) are a powerful tool for signal analysis. Compared to traditional Fourier techniques, time-frequency analysis is well-known to be more versatile and informative when dealing with phenomena whose spectral content is time-varying. The first algorithm of this paper, the MPD time-frequency based damage classifier, combines Gabor-atom[16, 17] based MPD and the TFR known as the Wigner distribution[19] for the classification of structural damage based on correlations in the time-frequency plane with training data from various damage classes. The second algorithm, the modified matching pursuit decomposition (MMPD)[20–22] based damage classifier, attempts to classify damage by directly using the MPD with real experimental data for computing the size (energy) of the projections onto the damage classes.[22–24] The effectiveness of the proposed approach is demonstrated via results from an application to fastener damage classification.

The remainder of this paper is organized as follows. Section II briefly reviews the MPD and MMPD algorithms. In Section III we describe our time-frequency based damage classifiers. Section IV presents an application for the classification of fastener damage in an aluminum plate. This is followed by summary and conclusion in Section V.

II.   Matching Pursuit Decomposition

Matching pursuit decomposition (MPD) is an iterative decomposition of a given signal $x(t)$ in terms of a linear combination of normalized basis functions or "atoms" $\{g_i(t)\}_{i=0,\ldots,N-1}$ as

$$x(t) = \sum_{i=0}^{N-1} \alpha_i \, g_i(t) + r_N(t), \tag{1}$$

where α_i are the expansion coefficients, given by

$$\alpha_i = \int_{-\infty}^{\infty} r_i(t) \, g_i(t) \, dt, \ i = 0, \ldots, N-1, \tag{2}$$

and $r_i(t)$ denotes the residue function after an i-term decomposition (with $r_0(t) \equiv x(t)$). The atoms are designed to *match* certain components of interest in the given signal class, and are chosen from a dictionary one-at-a-time in an iterative fashion so as to maximize the magnitude of the projections $|\alpha_i|$ in (2) at each iteration. The dictionary is in general not an orthonormal set, but is required to be complete.[16] Convergence holds in the L^2 sense, i.e.

$$\lim_{N \to \infty} \|x(t) - \sum_{i=0}^{N-1} \alpha_i \, g_i(t)\| = 0, \tag{3}$$

where $\|\cdot\|$ is the 2-norm $\|\cdot\|_2$. In practical applications, the truncation limit (number of expansion terms N in (1)) is usually chosen such that the energy of the residue after N iterations is smaller than some pre-defined value. Note that the MPD by design (a) yields the best-fit (in the sense of maximizing each single-step projection) most compact representation of the given signal in terms of the chosen family of basis functions, and (b) effectively filters out unwanted signal components such as noise, because the noise subspace is typically orthogonal to that spanned by the dictionary elements (provided, of course, that the truncation limit N is chosen appropriately).

Two different types of matching pursuit dictionary atoms are employed in this work. The first kind has the form

$$g_i(t) = e^{-\kappa_i^2 \, (t-\tau_i)^2} \cos\left(2\pi f_i t\right), \tag{4}$$

normalized to unit energy. These are essentially time-shifted (by τ_i), frequency-shifted (by f_i), and scaled (by κ_i) Gaussian-window harmonics. There are several advantages of using Gaussian time-frequency atoms.[16] First, they fit naturally into the TFR framework above. In fact, closed-form analytical expressions are

available[16, 17] for the TFRs of such atoms (in particular, the Wigner distribution of the Gaussian time-frequency atoms is also known to be Gaussian[19]). Gaussian atoms are also attractive from an information-theoretic point of view because, of all functions, Gaussians are the most concentrated in both time and frequency, and minimize the time-bandwidth product dictated by the uncertainty principle.[19] The second kind of dictionary employed here is composed of time- and frequency-shifted signals of real sensor data obtained from structural damage experiments. This approach is also referred to as the modified matching pursuit decomposition (MMPD).[20, 21] Because this kind of dictionary is matched specifically to the signals of interest in this application, it has the important advantage of yielding highly parsimonious representations.

III. Time-Frequency Damage Classifier

In this section, we describe the time-frequency based structural damage classifiers.

A. MPD Time-frequency based Damage Classifier

Starting with the MPD of the received signals, the time-frequency based algorithm effects classification by comparison (via correlation) of the cross-term free TFR[16] in the time-frequency plane

$$\mathscr{E}(t,f) = \sum_{i=0}^{N-1} |\alpha_i|^2 \, \mathrm{WD}_{g_i}(t,f), \tag{5}$$

where WD denotes the Wigner distribution,[19] given for a signal $x(t)$ by

$$\mathrm{WD}_x(t,f) = \int_{-\infty}^{\infty} x\left(t + \frac{\tau}{2}\right) x^*\left(t - \frac{\tau}{2}\right) e^{-j2\pi f\tau} \, d\tau. \tag{6}$$

Note that the cross-term free TFR is computed directly from the signal MPD. Note, furthermore, that the TFR can be computed analytically because the Wigner distribution of the Gabor dictionary atoms $g_i(t)$ are known in closed form.[19] The strength of correlations in the time-frequency plane is used to quantify how similar or dissimilar a given test signal is to members of known damage classes, and the test object declared to be from the class which maximizes the correlation. To be precise, a given test signal $x(t)$ is assigned to the class:

$$j = \arg\max_{i \in \Lambda} \frac{1}{M_i} \sum_{k=1}^{M_i} \left| \int_{-\infty}^{\infty} \int_{-\infty}^{\infty} \hat{E}_x(t,f) \, \hat{E}_{y_i^k}(t,f) \, dt \, df \right|, \tag{7}$$

where y_i^k denotes the kth training signal from class i, M_i is the number of training signals in class i, and Λ is the set of all classes. The $\hat{}$ is used to indicate that the TFRs are normalized to unit energy before the computation of the inner product.

B. Modified Matching Pursuit Decomposition (MMPD) based Damage Classifier

The MMPD based damage classifier classifies structural damage by directly using the MPD with real sensor data obtained from structural damage experiments as atoms for computing the size (energy) of the projections onto the damage classes.[22–24] In this framework, a given test signal $x(t)$ is assigned to the class:

$$j = \arg\max_{i \in \Lambda} \sum_{k=0}^{N-1} |\alpha_k|^2 \, \delta_{C_k, i}, \tag{8}$$

where α_k is the kth MPD expansion coefficient of signal $x(t)$, C_k is class to which the atom selected in the kth iteration belongs, δ denotes the Kronecker delta symbol, and Λ is the set of all classes. The delta term restricts the summation over k to only those atoms which belong to class i. This yields the size of the projection of the test signal $x(t)$ onto the atoms selected from class i, which is then used for classifying $x(t)$.

IV. Application to Fastener Damage Classification

In this section, we describe an application of the proposed time-frequency based structural damage classifiers for the classification of fastener damage in an aluminum plate.

A. Experimental Setup and Data Collection

The data concerns fastener failure (loose bolt) experiments conducted at the Advanced Structural Concepts Branch, Air force Research Lab. The test article is a 12 inch by 12 inch by 0.204 inch four-bolt aluminum plate[25] with four surface mounted piezoelectric transducers (PZT-1, 2, 3 and 4) of diameter 0.25 inch (see Figure 1). PZT-1 acts as the actuator while the remaining three serve as sensors. The excitation signal is a 0-1.5 KHz swept frequency sinusoid (all signals sampled at 5KHz) and induces normal structural vibrations. Any change in the structural dynamics would reflect on the modal response in terms of frequency shift and damping.
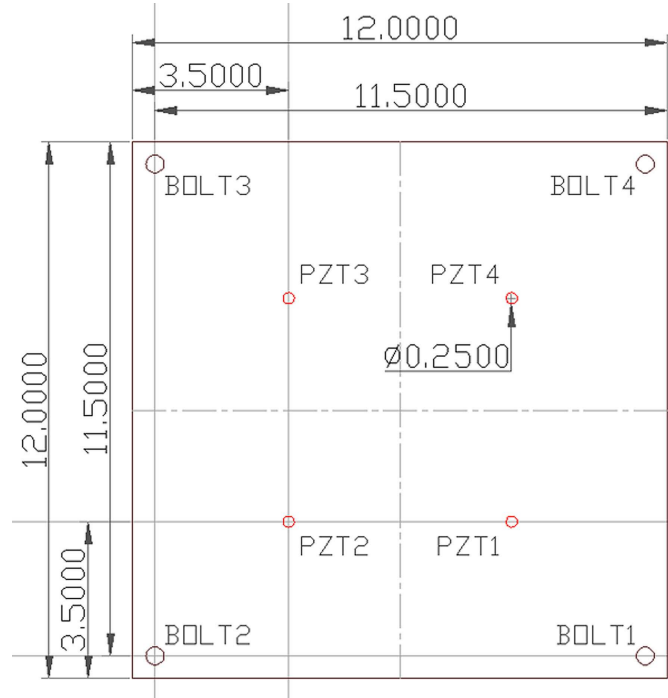

Figure 1. Experimental setup for fastener damage in a square aluminum plate[25] (all dimensions in inches).

Data was collected in several rounds, and comprises the responses from PZT-2, 3 and 4 for the five different structural conditions corresponding to one of the bolts being at 25% torque (30 inch-pound) or all bolts being at 100% torque (120 inch-pound). This gives rises to five different structural conditions (classes) for classification, the latter being the healthy case. Altogether, from each of the three receivers, we have 400 signals each for the first four structural conditions and 1,600 for the last one. Figure 2(a) shows example plots of the signal transmitted by PZT-1 and Figures 2(b)-2(f) show the signals received by PZT-3 for the five classes.

B. Preprocessing and Matching Pursuit Decomposition

The measured signals were first mean-centered, normalized, and time-aligned. Signal decomposition was then carried our using MPD and MMPD as described in Section II.

For the time-frequency damage classifier, the MPD was carried out to $K = 60$ iterations for each waveform with a dictionary composed of about 42 million normalized time-frequency Gabor atoms spanning 0 to 2 sec in time and 0-2.5 KHz in frequency. Figures 3(b)-3(f) show example plots of PZT-3 preprocessed signals for the five classes after 60 iterations of MPD. Figure 3(a) shows the residual signal energy versus MPD iteration number K. The residual energy decreases as K increases. Note that the choice $K = 60$ corresponds to a residual energy of about 20 %. The atoms in the MPD of each signal are characterized by the parameters κ_i, τ_i, f_i (eq. (4)), and the expansion coefficients α_i (eq. (2)), for $i = 0, \ldots, K - 1 = 59$.

Figure 4(a) shows the Wigner distribution (magnitude) of the excitation chirp signal and Figures 3(e)-4(f) show the cross-term free TFR (eq. (5)) for the example class 4 signal considered earlier. We observe that

(a) Transmitted signal (PZT-1)

(b) Class 1 received signal (PZT-3)

(c) Class 2 received signal (PZT-3)

(d) Class 3 received signal (PZT-3)

(e) Class 4 received signal (PZT-3)

(f) Class 5 received signal (PZT-3)
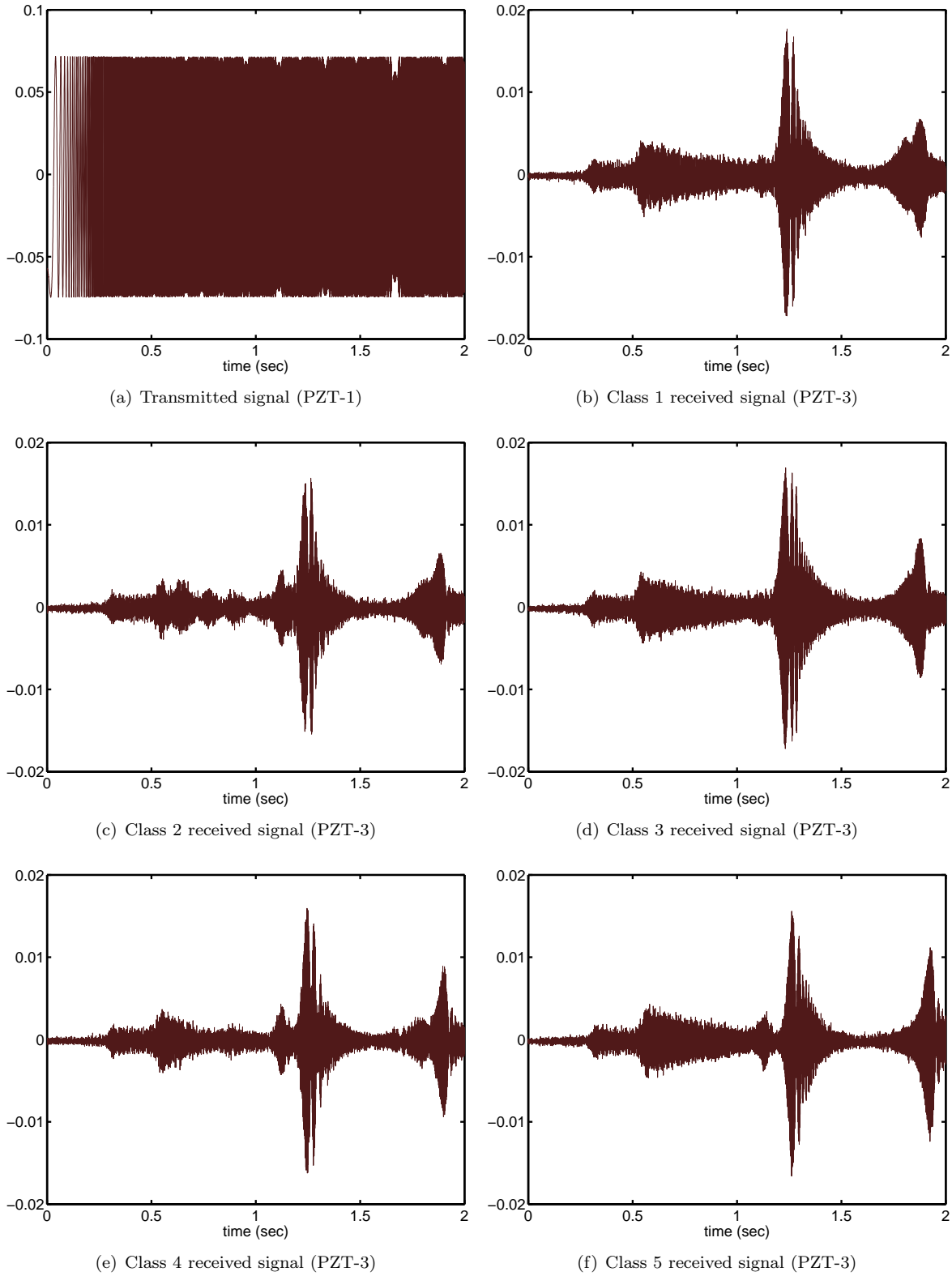
Figure 2. Example plots showing the signal transmitted by PZT-1 and the signals received by PZT-3 for the five classes.

American Institute of Aeronautics and Astronautics

48th AIAA/ASME/ASCE/AHS/ASC Structures, Structural Dynamics, and Materials Conference
23 - 26 April 2007, Honolulu, Hawaii

AIAA 2007-2055
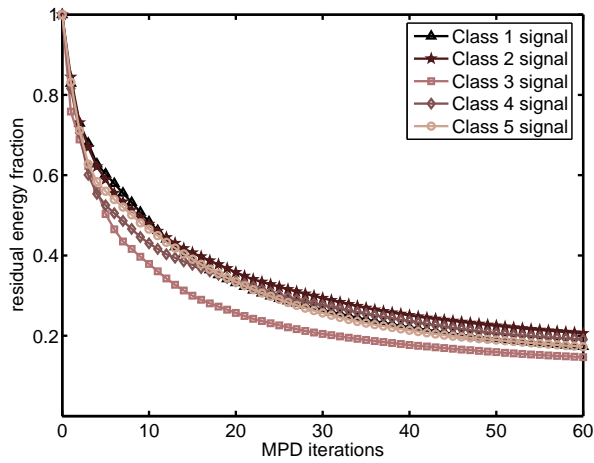
(a) Residual signal energy vs. MPD iteration no.
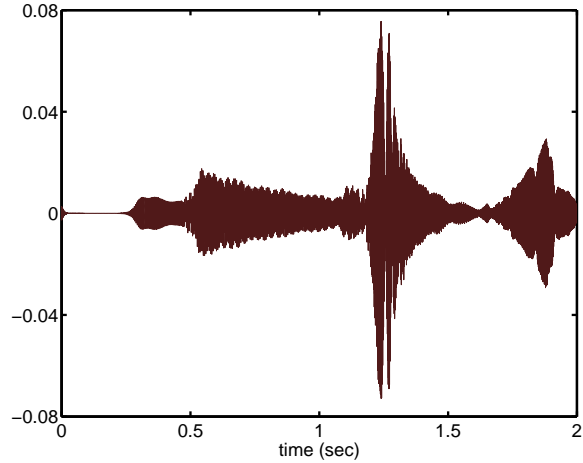
(b) Class 1 signal after 60 MPD iterations (PZT-3)
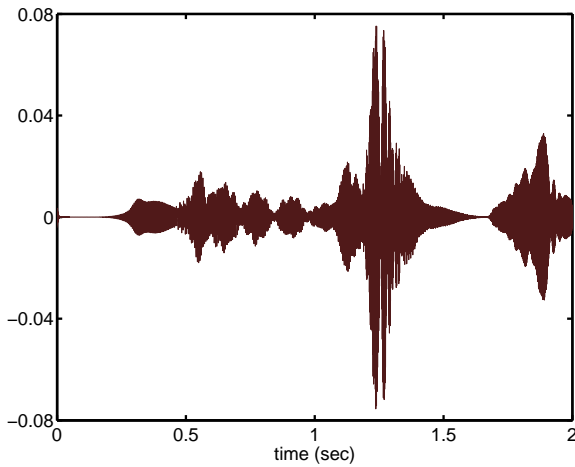
(c) Class 2 signal after 60 MPD iterations (PZT-3)
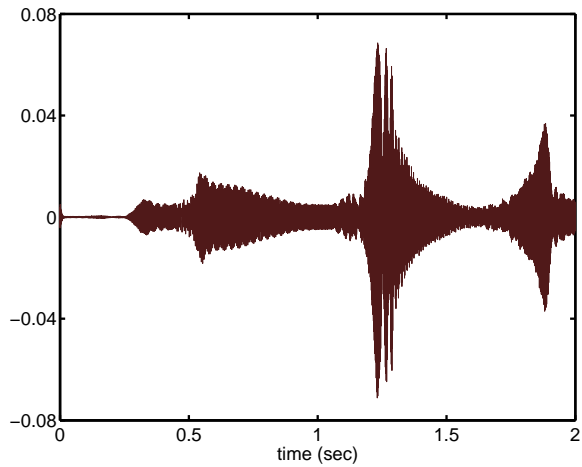
(d) Class 3 signal after 60 MPD iterations (PZT-3)
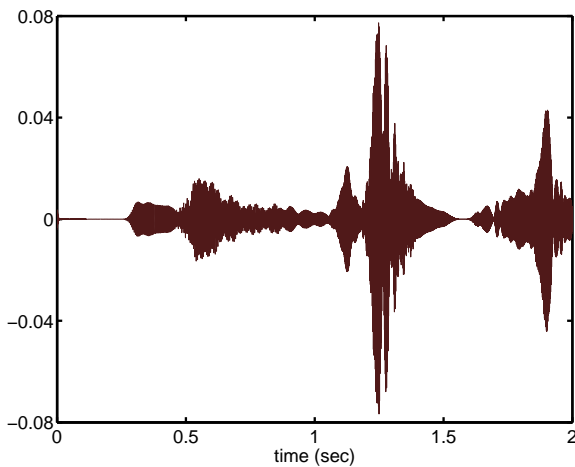
(e) Class 4 signal after 60 MPD iterations (PZT-3)
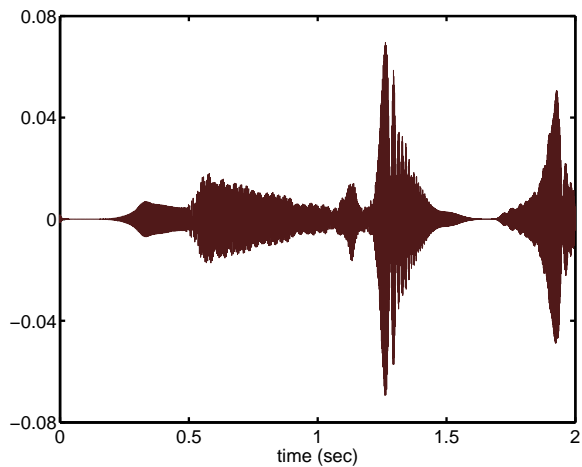
(f) Class 5 signal after 60 MPD iterations (PZT-3)

Figure 3. Example plots showing the residual signal energy versus MPD iteration number, and the PZT-3 signals for the five classes after preprocessing and 60 MPD iterations.

American Institute of Aeronautics and Astronautics

48th AIAA/ASME/ASCE/AHS/ASC Structures, Structural Dynamics, and Materials Conference
23 - 26 April 2007, Honolulu, Hawaii

AIAA 2007-2055

there are some atoms that dominate the TFR and appear at about the same place on the time-frequency plane.

Investigation of the MPD of the various waveforms revealed that the atoms that are selected in the first three iterations $K = 1, 2, 3$ are characterized by frequency and time-shifts common to all the waveforms irrespective of class. Figure 5 shows that the peak of the waveforms from various classes (solid lines) lie in the same spectral region as is denoted by the first three MPD atoms (dotted lines). Based on this observation, the first three atoms (that contain most of the wave energy) were removed before subsequent processing to enhance the sensitivity of the classifier to finer details (lower energy components) unique from one class of defect to another. Preliminary FEM analysis confirms that these were the natural frequencies of the test specimen.

In the case of the MMPD based damage classifier, only $K = 10$ MMPD iterations were needed for reducing the residue energy to about 20-30 % of the signal energy (see Figure 6). This is because the dictionary composed of time and frequency-shifted real data was better matched to the waveforms being decomposed. Frequency shifts from 0 to 25 Hz in steps of 0.25 Hz were found to be sufficient in this case.

Since the MPD (and MMPD) dictionary is composed mainly of elements which are time and frequency translates of one another, the projections α_i in (2) are nothing but convolutions in time and frequency. These were therefore evaluated with great efficiency using the fast Fourier transform (FFT). The MPD algorithm was implemented in C making use of parallel programming capability provided by Message Passing Interface (MPI). A computing cluster comprised of seven 3 GHz dual-core Intel Pentium D processors running Linux (with 2 GB RAM each) was employed for performing the simulations. In the case of MPD algorithm, the Gabor atoms were constructed in the frequency domain directly using an analytical formula to save the one-time cost of Fourier transforming the entire dictionary.

The parallelization efficiency of the MPD implementation is demonstrated in Figure 7. The run-time T was modeled as a function of the number of processors using the linear model

$$T = c_1 + c_2 \frac{N_w}{N_p}, \tag{9}$$

where c_1 is the pre-computation cost common to all the nodes, c_2 is the (per waveform) computational cost of the parallelizable part of the code, N_w is the total number of waveforms and N_p is the number of processing cores. The small discrepancy between the actual run-times and those predicted by the model is due to the fact that this model does not account for communication cost and network delays.

C.   Classification Results

For the MPD time-frequency based damage classifier, half of the data set was used for training (estimating the template TFRs for each class) and half for testing the classifier performance. The performance of the classifier is quantified here by means of a 5×5 confusion matrix. Essentially, the (i, j)th element of this matrix indicates the probability that data from class i is classified as being from class j. Ideally, this would be a 5×5 identity matrix. For our time-frequency based structural damage classifier, we obtain the confusion matrix:

$$\begin{bmatrix} 0.760 & 0 & 0.240 & 0 & 0 \\ 0.030 & 0.930 & 0 & 0.025 & 0.015 \\ 0 & 0 & 1.000 & 0 & 0 \\ 0 & 0.015 & 0 & 0.975 & 0.010 \\ 0 & 0 & 0 & 0 & 1.000 \end{bmatrix}. \tag{10}$$

We find that the performance of the classifier is good (the average percentage correct classification is more than 90%), demonstrating the utility of this approach.

For the MMPD based damage classifier, we used 20 waveforms from each class to build the dictionary of the MMPD algorithm. The performance of the classifier on a randomly selected different set of waveforms

American Institute of Aeronautics and Astronautics

48th AIAA/ASME/ASCE/AHS/ASC Structures, Structural Dynamics, and Materials Conference 23 - 26 April 2007, Honolulu, Hawaii

AIAA 2007-2055
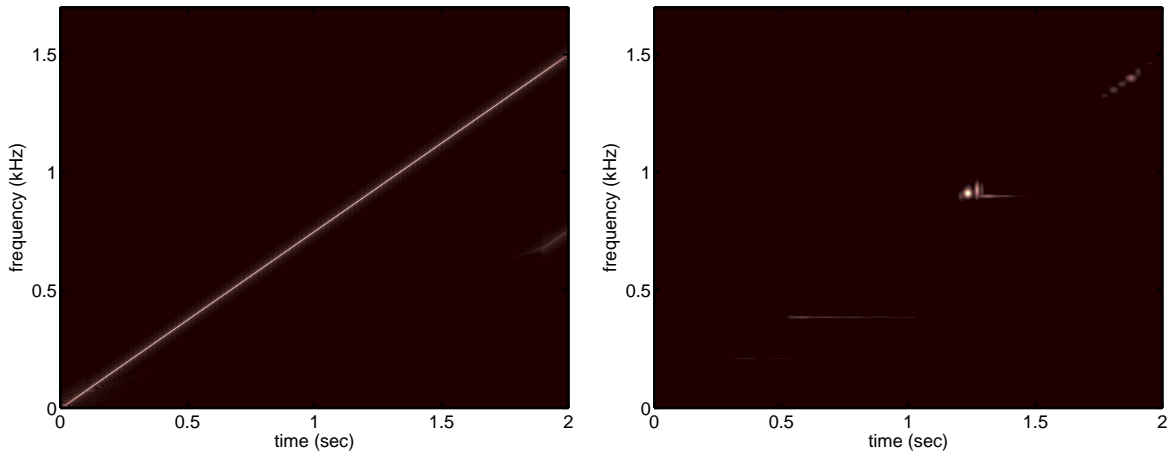
(a) Wigner distribution of transmitted signal (PZT-1)

(b) TFR of class 1 signal after 60 MPD iterations (PZT-3)
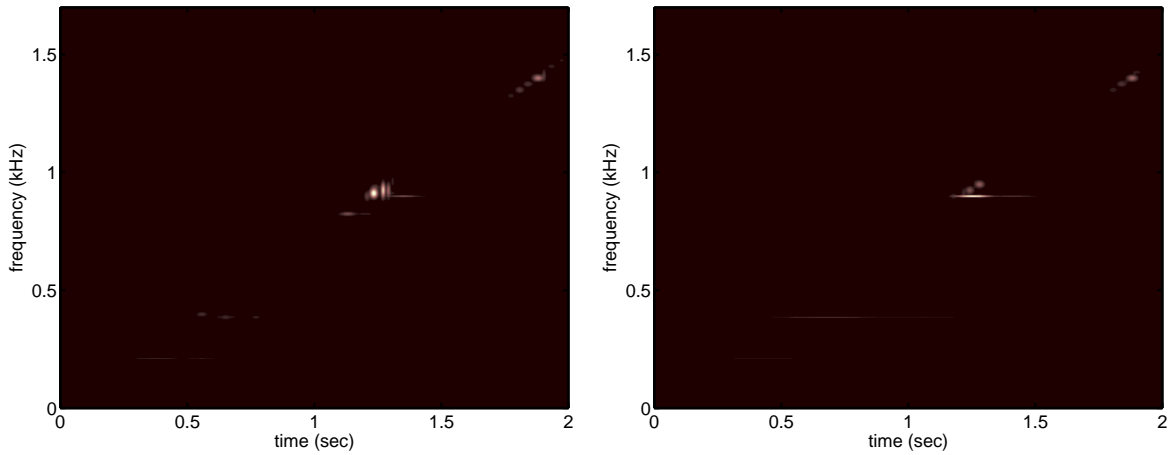
(c) TFR of class 2 signal after 60 MPD iterations (PZT-3)

(d) TFR of class 3 signal after 60 MPD iterations (PZT-3)
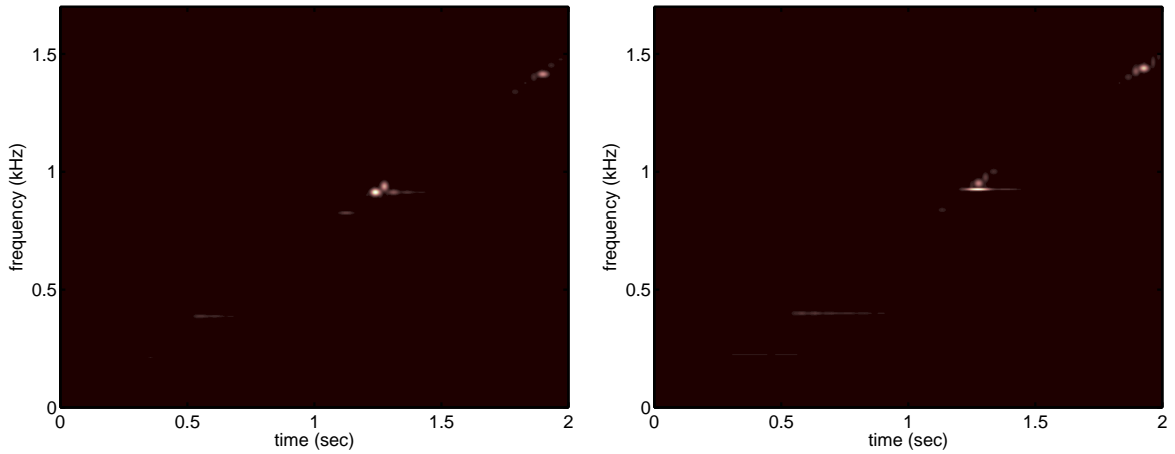
(e) TFR of class 4 signal after 60 MPD iterations (PZT-3)

(f) TFR of class 5 signal after 60 MPD iterations (PZT-3)

Figure 4. Example plots showing the Wigner distribution (magnitude) of the transmitted signal and TFRs of the five classes after preprocessing and 60 MPD iterations.

American Institute of Aeronautics and Astronautics

48th AIAA/ASME/ASCE/AHS/ASC Structures, Structural Dynamics, and Materials Conference
23 - 26 April 2007, Honolulu, Hawaii

AIAA 2007-2055
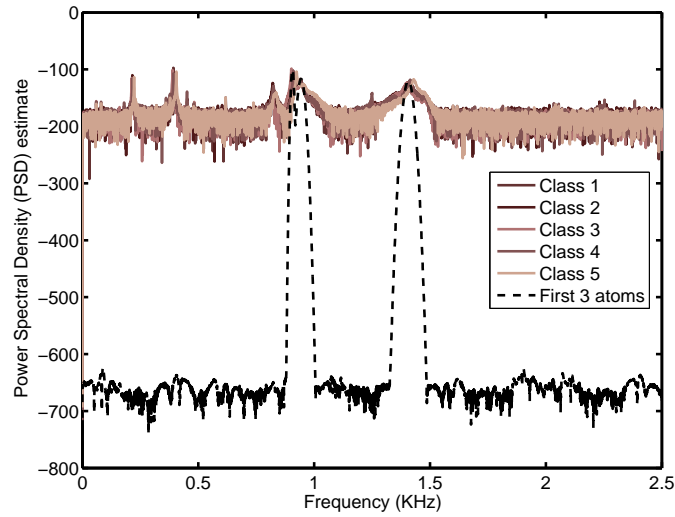
Figure 5. PSD of a few waveforms from each of the 5 classes and reconstruction using 3 MPD atoms.

(a) Class 4 signal after 10 MMPD iterations (PZT-3)

(b) Residual signal energy vs. MMPD iteration no.
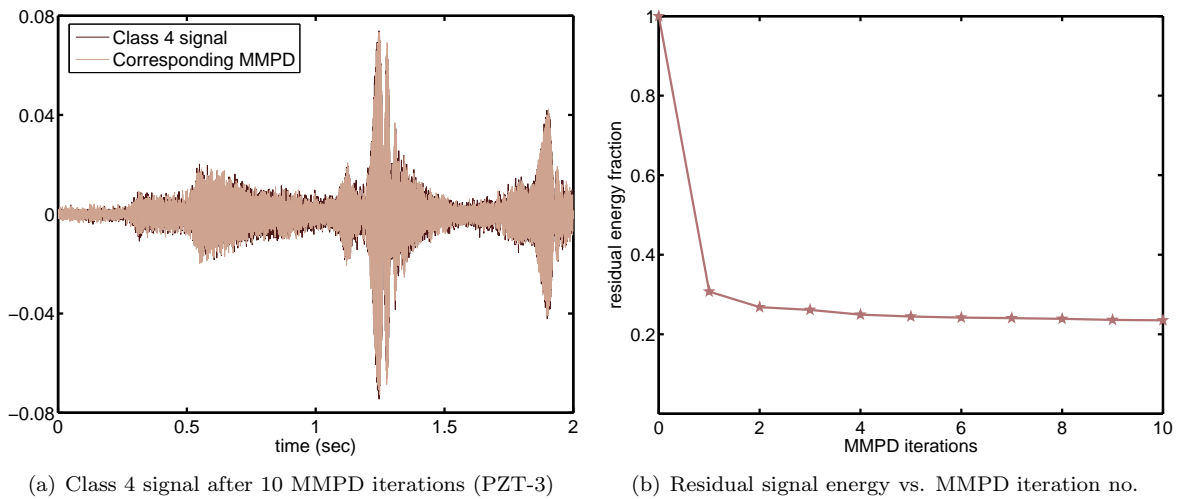
Figure 6. Example plots showing a class 4 PZT-3 signal after preprocessing and 10 MMPD iterations, and the residual signal energy versus MMPD iteration number.

American Institute of Aeronautics and Astronautics
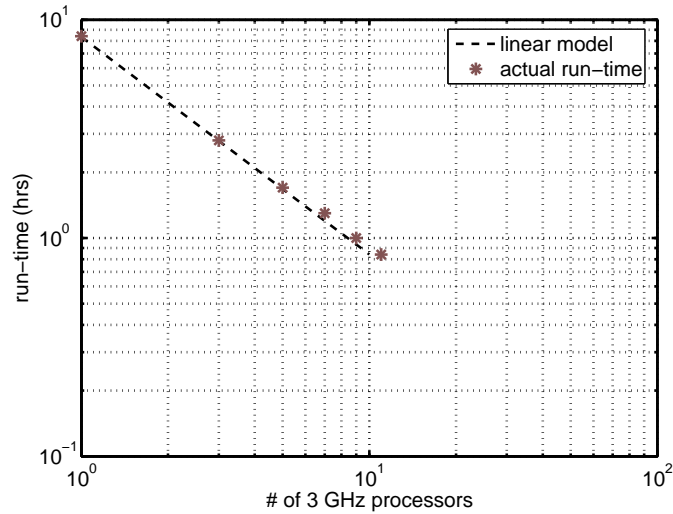
Figure 7. Parallelization efficiency of the MPD implementation.

(20 from each class) is shown in the confusion matrix below:

$$\begin{bmatrix} 20 & 0 & 0 & 0 & 0 \\ 0 & 20 & 0 & 0 & 0 \\ 0 & 0 & 20 & 0 & 0 \\ 0 & 0 & 0 & 20 & 0 \\ 0 & 0 & 0 & 0 & 20 \end{bmatrix}. \tag{11}$$

Not a single mis-classification was observed in the set of data tested.

V.   Conclusion

In this paper, we have presented the MPD and MMPD time-frequency based algorithms for the classification of structural damage. When applied to the classification of fastener damage in an aluminum plate, we find that the MPD time-frequency classifier yields an average percentage correct classification rate of over 90% while the MMPD based classifier yields 100 % correct classification rate. This performance of the former can be further improved as follows. Firstly, the time-frequency MPD dictionary employed in the first algorithm is based on Gabor atoms. Fully $K = 60$ MPD iterations are needed to bring the residual energy to about 20%. In order to make the decomposition more efficient we plan to investigate a dictionary that uses chirps instead of Gabor functions. Since chirps are better-matched to the signals of interest here, we expect faster convergence of the MPD (smaller K for a given residue) and consequently savings in computational costs. Also, our present simulations only consider data collected from PZT-3 for simplicity. We next plan to address sensor fusion, where the full data-set including signals obtained from the other sensors is utilized for achieving optimal classification performance. Results of these studies will be reported in subsequent publications.

Acknowledgments

American Institute of Aeronautics and Astronautics

48th AIAA/ASME/ASCE/AHS/ASC Structures, Structural Dynamics, and Materials Conference
23 - 26 April 2007, Honolulu, Hawaii

AIAA 2007-2055

References

[1]Lepine, B., Wallace, B., Forsyth, D., and Wyglinski, A., "Pulsed Eddy Current Method Developments for Hidden Corrosions Detection in Aircraft Structures," *Proceedings of the 1st Pan-American Conference for NDT*, Toronto, Canada, 1998, pp. 118–124.

[2]Schoess, J., "Development and Application of Stress-Wave Acoustic Diagnostic for Roller-Bearings," Tech. rep., Honeywell Tech. Center Report, 1999.

[3]Fotos, C., "Acoustic Emission Technique Tests Aircraft Integrity," *Aviation Week & Space Technology*, Vol. 28, No. 76, 1989.

[4]Mcbride, S., Viner, M., Pollard, M. D., MacPhail, P. S., and Peters, D. T., "Acoustic Emission Detection of Crack Presence and Crack Advance During Flight," *AGARD-CP-462*, 1989.

[5]Gelman, L., Giurgiutiu, V., and Petrunin, I., "Advantage of using the Fourier components pair instead of power spectral density for fatigue crack diagnostics," *International Journal of COMADEM*, Vol. 7, 2004, pp. 18–22.

[6]Jeong, H. and Jang, Y.-S., "Fracture Source Location in Thin Plates Using the Wavelet Transform of Dispersive Waves," *IEEE Transactions on Ultrasonics, Ferroelectrics, and Frequency Control*, Vol. 47-3, 2000, pp. 612–619.

[7]Eren, L. and Devaney, M. J., "Bearing Damage Detection via Wavelet Packet Decomposition of the Stator Current," *IEEE Transactions on Instrumentation and Measurement*, Vol. 53-2, 2004, pp. 431–436.

[8]Sun, A. and Chang, C. C., "Statistical wavelet-based method for structural health monitoring," *Journal of structural engineering*, 2004, pp. 1055–1062.

[9]Sohn, H., Farrar, C. R., Hunter, N. F., and Worden, K., "Structural Health Monitoring Using Statistical Pattern Recognition Techniques," *Transactions of the ASME*, Vol. 123, 2001, pp. 706–711.

[10]Nguyen, M., Wang, X., Su, Z., and Ye, L., "Damage Identification for Composite Structures with a Bayesian Network," *ISSNIP*, 2004, pp. 307–312.

[11]Sohn, H., Allen, D. W., Worden, K., and Farrar, C. R., "Structural Damage Classification Using Extreme Value Statistics," *Journal of Dynamic Systems, Measurement, and Control*, Vol. 127, 2005, pp. 125–132.

[12]Guo, N. and Cawley, P., "Lamb Wave Reflection for the Quick Non-Destructive Evaluation of Large Composite Laminates," *Material Evaluation*, Vol. 52, 1994, pp. 404–411.

[13]Pierce, S. G., Philp, W. R., Culshaw, B., Gachagan, A., McNab, A., Hayward, G., and Lecuyer, F., "Surface-Bonded Optical Fiber Sensors for the Inspection of CFRP Plates Using Ultrasonic Lamb Waves," *Smart materials and Structures*, Vol. 5, 1996, pp. 776–787.

[14]Jansen, D. P., Hutchins, D. A., and Mottram, J. T., "Lamb Wave Tomography of Advanced Composite Laminates Containing Damage," *Ultrasonics*, Vol. 32, 1994, pp. 83–89.

[15]Giurgiutiu, V., "Tuned Lamb Wave Excitation and Detection with Piezoelectric Wafer Active Sensors for Structural Health Monitoring," *Journal of Intelligent Material Systems and Structures*, Vol. 16, 2005, pp. 291–305.

[16]Mallat, S. G. and Zhang, Z., "Matching pursuits with time-frequency dictionaries," *IEEE Trans. on Signal Processing*, Vol. 41, December 1993, pp. 3397–3415.

[17]Papandreou-Suppappola, A. and Suppappola, S. B., "Analysis and Classification of Time-Varying Signals with Multiple Time-Frequency Structures," *IEEE Signal Processing Letters*, Vol. 9, 2002, pp. 92–95.

[18]Das, S., Papandreou-Suppappola, A., Zhou, X., and Chattopadhyay, A., "On the Use of the Matching Pursuit Decomposition Signal Processing Technique for Structural Health Monitoring," *12th SPIE Annual International Symposium on Smart Structures and Materials, Paper 5764-65*, San Diego, CA, 2005.

[19]Papandreou-Suppappola, A., editor, *Applications in Time-Frequency Signal Processing*, CRC Press, Florida, 2002.

[20]Papandreou-Suppappola, A. and Suppappola, S. B., "Adaptive time-frequency representations for multiple structures," *Proc. 10th IEEE Workshop on Statistical Signal and Array Processing*, Vol. 3, Pocono Manor, PA, 2000.

[21]Papandreou-Suppappola, A. and Suppappola, S. B., "Analysis and classification of time-varying signals with multiple time-frequency structures," *IEEE Signal Processing Letters*, Vol. 9, 2002, pp. 92–95.

[22]Ebenezer, S. P., Papandreou-Suppappola, A., and Suppappola, S. B., "Classification of Acoustic Emissions Using Modified Matching Pursuit," *EURASIP Journal on Applied Signal Processing*, Vol. 3, 2004, pp. 347357.

[23]Ebenezer, S. P., *Classification of time-varying signals from an acoustic monitoring system using time-frequency techniques*, Master's thesis, Arizona State University, Tempe, AZ, December 2001.

[24]Ebenezer, S. P., Papandreou-Suppappola, A., and Suppappola, S. B., "Matching pursuit classification for time-varying acoustic emissions," *35th Asilomar Conference on Signals, Systems and Computers*, 2001, pp. 715–719.

[25]Olson, S. E., DeSimio, M. P., and Derriso, M. M., "Fastener Damage Estimation in a Square Aluminum Plate," *Structural Health Monitoring*, Vol. 5, 2006, pp. 173–183.

American Institute of Aeronautics and Astronautics